Article

Topological Study of the First Step of Nucleophilically Unassisted Solvolysis of Protonated 2-*Endo/Exo*-Norbornanol and Protonated 2-*Endo/Exo*-Oxabicycloheptanol

Caio L. Firme,§*

Instituto de Química, Universidade Federal do Rio de Janeiro, Av. Athos da Silveira Ramos, 149,
CT Bloco A, Cidade Universitária, Ilha do Fundão, 21941-909 Rio de Janeiro-RJ, Brazil

A assistência da deslocalização de elétrons sigma ou assistência anquimérica dos elétrons sigma explica grandes diferenças de velocidade na solvólise de 2-*exo*- e 2-*endo*-norbornil-*p*-bromobenzenosulfonatos. Este estudo foi anteriormente analisado pela teoria dos orbitais moleculares em fase gás. Ao revisitar este antigo problema a partir da teoria quântica de átomos em moléculas (QTAIM), novas informações sobre essas reações foram obtidas. Os resultados de QTAIM mostram que, na primeira etapa da solvólise não assistida nucleofilicamente dos alcoóis protonados 2-*exo*-norbornanol e 2-*endo*-norbornanol, ambas as reações são anquimericamente assistidas pela participação de elétrons sigma. Similarmente, na primeira etapa da solvólise não assistida nucleofilicamente dos álcoois protonados 2-*endo*-oxabiciclcloheptanol e 2-*exo*-oxabiciclcloheptanol, os resultados de QTAIM mostram que ambas as reações são anquimericamente assistidas: a primeira a partir da participação da ligação sigma C–O e de pares de elétrons isolados do oxigênio e a última a partir da participação da ligação sigma C1–C2.

The assistance of σ electron delocalization or anchimeric assistance of σ electrons accounts for the large rate differences in the solvolysis of 2-*exo*- and 2-*endo*-norbornyl-*p*-bromobenzenesulfonates. This study was formerly analyzed by molecular orbital theory in gas phase. By revisiting this old problem from the quantum theory of atoms in molecules (QTAIM), new information on these reactions was obtained. The QTAIM results show that, in the first step of the nucleophilically unassisted solvolysis of protonated 2-*exo*-norbornanol and of protonated 2-*endo*-norbornanol, both reactions are anchimerically assisted by sigma bond participation. Similarly, in the first step of the nucleophilically unassisted solvolysis of protonated 2-*endo*-oxabicycloheptanol and of protonated 2-*exo*-oxabicycloheptanol, the QTAIM results show that both reactions are anchimerically assisted: the former from sigma bond participation from O–C bonds and valence shell electron participation from oxygen atom and the latter from sigma bond participation from C1–C2 bond.

Keywords: QTAIM, 2-norbornyl cation, sigma bond participation, 2-oxabicycloheptanol, solvolysis
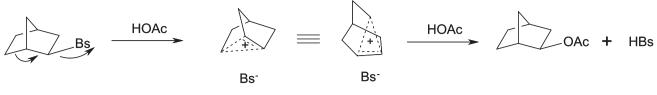
Introduction

The assistance of σ electron delocalization[1] or anchimeric assistance of σ electrons[2-4] accounts for the large rate differences in the solvolysis of 2-*exo*- and 2-*endo*-norbornyl-*p*-bromobenzenesulfonates.[5-8] Different experimental approaches indicated the influence of anchimeric assistance on the solvolysis of 2-*exo*-norbornyl tosylate.[9-14] In addition, it was established the nucleophilically unassisted character of 2-*exo*-norbornyl tosylate solvolysis.[9,15,16]

On the other hand, Brown *et al.*[17,18] attributed the large rate differences in the solvolysis of 2-*exo/endo*-norbornyl derivatives to steric effects. Thereafter, heated debates on nature of 2-norbornyl cation, named the nonclassical ion controversy, took place.[17-19]

Winstein *et al.*[5-7] postulated the nonclassical structure of 2-norbornyl cation, later proved by experimental evidences,[20-25] as intermediate in the solvolysis of 2-*exo*-norbornyl brosilate (Scheme 1). However, Winstein[26]

*e-mail: caiofirme@quimica.ufrn.br; firme.caio@gmail.com
§Present address: Instituto de Química, Universidade Federal do Rio Grande do Norte, Av. Salgado Filho s/n, Lagoa Nova, 59072-970 Natal-RN, Brazil

Scheme 1.

was aware that "carbon bridging lags behind ionization at the transition state" in the solvolysis of 2-norbornyl derivatives. Winstein[26] reasoned that Brown *et al.*[17,18] was interpreting incorrectly Hammond's postulate when argued that the transition state for ionization of 1-substituted and 2-substituted norbornyl systems to a bridged ion should closely resemble the latter. Winstein affirmed that "carbon bridging lags behind ionization at the transition state" in the solvolysis of 2-norbornyl derivatives, which means that the amount of stabilization due to delocalization in the free ion is much larger than in the transition state. Some experimental methods[27,28] showed that the carbon bridging from C6–C1 bond does not affect very much the transition state in the solvolysis of 2-norbornyl derivatives.

Schleyer and co-workers[29] in late 70's and Mueller *et al.*[30] in early 90's postulated that 90% of the carbocation character is developed in the solvolysis transition states, which could contradict the aforementioned Winstein's hypothesis.[26] As a consequence of early conclusions from Schleyer and co-workers[29] and those from Mueller *et al.*[30] (similarity of carbocation character between free ion and transition state), it was expected that the energy difference between the classical 2-norbornyl cation (without carbon bridging) and the nonclassical 2-norbornyl cation (with carbon bridging) was similar to the energy difference of the transition state on the solvolysis of 2-*endo*-norbornyl derivative (without carbon bridging) and the transition state on the solvolysis of 2-*exo*-norbornyl derivative (with carbon bridging). However, this similarity does not exist[31-33] and Schleyer and co-workers[33] eventually proved Winstein´s hypothesis[26] for some 2-norbornyl derivatives.

The quantum theory of atoms in molecules[34,35] (QTAIM) has been used to study the electronic nature of norbornyl cation and derivatives.[36-39] In this work, we applied QTAIM to reevaluate the first step of two unassisted nucleophilic solvolysis: $[R–OH_2]^+ \rightarrow R^+ + H_2O$, where R is 2-*endo/exo*-norbornyl and 2-*endo/exo*-oxabicycloheptanyl moieties, that were previously studied by Schleyer and co-workers[33] by using molecular orbital theory. Certainly, different leaving groups would lead to different carbocation character to the transition state structure of the studied molecules in gas phase, but our work is restricted to water as leaving group for comparison reasons with the work of Schleyer and collaborators.[33] In the light of QTAIM study, new and important information on

the first step of the studied reactions was drawn. This work highlights the importance of revisiting old problems mainly when changing an orbital-based theoretical analysis into an observable-based theoretical analysis.

Methodology

Computational methods

The geometries of the studied species were optimized by using standard techniques.[40] Vibrational analyses on the optimized geometries of selected points on the potential energy surface were carried out to determine whether the resulting geometries are true minima or transition states, by checking the existence of imaginary frequencies. Calculations were performed at PBE1PBE/6-311++G** level[41,42] by using Gaussian 03 package.[43] Electronic density was obtained at PBE1PBE /6-311++G** level for further QTAIM calculations. All topological data were calculated by means of AIM2000 software.[44]

Quantum theory of atoms in molecules (QTAIM)

The quantum theory of atoms in molecules was developed by Bader in the early 70´s.[45-50] Bader's theory is known as the quantum theory of subsystem because atomic properties can be directly obtained from bonded atoms in a molecule, something that no other quantum mechanical theory is able to.[51] QTAIM relies on the accuracy of the theoretical method used to obtain the electron density matrix (wave function file) which is subsequently used by QTAIM to calculate the gradient of charge density of the studied molecular system in order to find critical points of the charge density. The critical points of the charge density function are found wherever the gradient of the charge density function is equal to zero ($\nabla\rho = 0$).

Several topological information can be obtained from the bond critical points (BPCs) and can be used to characterize a chemical bond or chemical interaction.[35] From a bond critical point, one can obtain, for example, the charge density at BCP (ρ_b), the Laplacian of the charge density at BCP ($\nabla^2\rho_b$) and the ellipticity (ε).

The Laplacian of the charge density represents the concentration or the depletion of the charge density in a

specific region of the molecular system.[35] The negative sign of $\nabla^2\rho$ represents the concentration of the charge density and the positive sign of $\nabla^2\rho$ represents charge depletion, *i.e.*, when $\nabla^2\rho_b < 0$ there is charge concentration in that BCP and when $\nabla^2\rho_b > 0$ there is charge depletion in that BCP.

The ellipticity (ε) gives the information about the cylindrical symmetry of a chemical bond. When ellipticity is zero or near zero, it means that the chemical bond has cylindrical symmetry such as in single bond or triple bond. When $\varepsilon \neq 0$, it means that the corresponding chemical bond has a formal bond order (n) in the range of near single bond to near triple bond ($1 < n < 3$), depending on its value.

The ratio $|\lambda_1|/\lambda_3$ is also obtained at the BCP and, in conjunction with other parameters, is used to classify chemical bonds. When the ratio $|\lambda_1|/\lambda_3 > 1$, it indicates a shared interaction in an atomic pair where the BCP is located, and when the ratio $|\lambda_1|/\lambda_3 << 1$, it indicates a closed shell interaction. Closed shell interactions are characteristic of ionic bonds and van der Waals interactions and shared interactions are characteristic of covalent bonds.[35]

The delocalization index (DI) is the amount of shared electrons between each atomic pair.[47,52] The higher DI value, the stronger is the interaction between a pair of atoms. From the charge density of the bond critical point is also possible to obtain the QTAIM bond order (n) or alternatively it may be directly obtained from the linear relation between DI and formal bond order.[53,54]
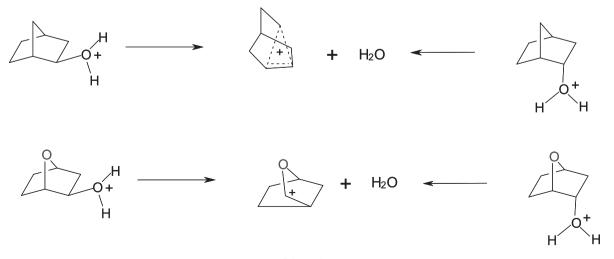
Results

The results of this work are restricted to gas phase in order to compare with previous gas phase results of Schleyer and co-workers[33] based on molecular orbital theory. They stated that both *endo/exo*-norbornyl tosylates undergo nucleophilically unassisted solvolysis in the first step of the reaction,[33] which means no solvent assistance in the first step. However, there is no evidence that *endo*-norbornyl tosylate is not solvent assisted in its solvolyis.[9] Since the present work is interested in the comparison of QTAIM and MO results, the calculations were done for the studied molecules in gas phase condition (*i.e.*, nucleophilically unassisted solvolysis).

Scheme 2 shows both reactions studied in this work, *i.e.*, the first step of nucleophilically unassisted solvolysis of protonated 2-*endo/exo*-norbornanol and protonated 2-*endo/exo*-oxabicycloheptanol.

Figure 1 shows a pictorial representation of the potential energy surface and the structures of protonated 2-*endo*- and 2-*exo*-norbornanol ground states (**1-GS** and **2-GS**, respectively), the corresponding transition states (**1-TS** and **2-TS**) and the intermediates (2-norbornyl cation and water) of the first step of the nucleophilically unassisted solvolysis. Figure 1 also shows the energy difference between 2-*endo/exo*-norbornanol ground states and the norbornyl cation and water intermediates [$\Delta G_{(GS-INT)}$] and corresponding activation energies (E_a) of the first step of the nucleophilically unassisted solvolysis. The activation energy difference of these reactions ($\Delta E_a = 4.27$ kcal mol^{-1}) is close to the corresponding value obtained by Schleyer and co-workers.[33]

Figure 2 shows the molecular graph of the transition state of the first step of the nucleophilically unassisted solvolysis of protonated 2-*endo*- and 2-*exo*-norbornanol. The molecular graph is a topological graph showing critical points and bond paths of the charge density function. There are three critical points in the molecular graphs below: nuclear attractor critical point, bond critical point (in red) and ring critical point (in yellow - see the online version).

Molecular graph of **1-TS** shows a bond path between oxygen atom of the leaving group and hydrogen atom
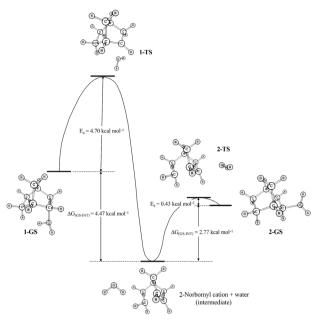

Scheme 2.

Figure 1. Pictorial representation of the potential energy surface (PES) and the energies of protonated 2-*endo*- and 2-*exo*- norbornanol ground states (**1-GS** and **2-GS**, respectively) relative to the energies of 2-norbornyl cation and water intermediates [$\Delta G_{(GS-INT)}$] of the first step of the nucleophilically unassisted solvolysis and their corresponding activation energies (E_a) along with the corresponding transition state structures (**1-TS** and **2-TS**, respectively).
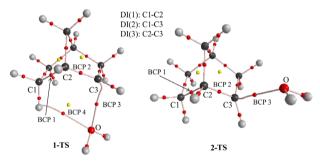

Figure 2. Molecular graph of the transition state of the first step of the nucleophilically unassisted solvolysis of protonated 2-*endo*- and 2-*exo*-norbornanol (**1-TS** and **2-TS**, respectively).

bonded to C1 atom. It represents a weak attractive interaction (see Table 1) between these atoms as indicated by Schleyer and co-workers.[33] This opposes Brown´s steric effects on the rate of the solvolysis of 2-*endo*-norbornyl derivatives.

Table 1 shows some geometrical (angle (degree) and bond length (Å)) and topological properties (charge density (ρ_b), Laplacian of charge density ($\nabla^2\rho_b$), atomic energy ($E_{at}(\Omega)$), sum of atomic energies of C1–C3 ($\Sigma E_{at}(\Omega)$), in a.u., ellipticity (ϵ) and the ratio $|\lambda_1|/\lambda_3$ of bond critical points) of the species **1-GS**, **2-GS**, **1-TS** and **2-TS**.

Figure 3 shows a pictorial representation of the potential energy surface and the energies of protonated 2-*endo*- and 2-*exo*-oxabicycloheptanol ground states (**3-GS** and **4-GS**) relative to the energies of oxabicycloheptanyl cation and
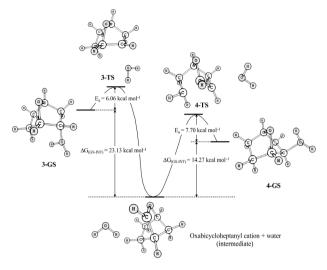

Figure 3. Pictorial representation of the PES and the energies of protonated 2-*endo*- and 2-*exo*-oxabicycloheptanol ground states (**3-GS** and **4-GS**, respectively) relative to the energies of the oxabicycloheptanyl cation and water intermediates [$\Delta G_{(GS-INT)}$] of the first step of the nucleophilically unassisted solvolysis and their corresponding activation energies (E_a) along with the corresponding transition state structures (**3-TS** and **4-TS**, respectively).

water intermediates of the first step of the nucleophilically unassisted solvolysis and their corresponding activation energies along with the corresponding transition state structures (**3-TS** and **4-TS**).

Figure 4 depicts the molecular graphs of the transition structures **3-TS** and **4-TS**. There is no interaction between the hydrogen atom (from norbornyl moiety) and the oxygen atom in **3-TS** and **4-TS**.
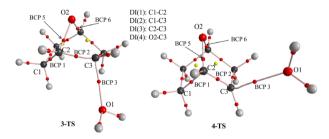

Figure 4. Molecular graph of the transition state of the first step of the nucleophilically unassisted solvolysis of protonated 2-*endo*- and 2-*exo*-oxabicycloheptanol (**3-TS** and **4-TS**, respectively).

Table 2 shows some geometrical information along with ρ_b, $\nabla^2\rho_b$, $E_{at}(\Omega)$, $q(\Omega)$, $\Sigma E_{at}(C1-C3)$, ϵ, $|\lambda_1|/\lambda_3$ of the bond critical points 1-3, 5 and 6, and DI of their corresponding atomic pairs of the species **3-GS**, **4-GS**, **3-TS** and **4-TS**.

Figure 5 shows the molecular graphs of the 2-norbornyl cation[36,38,39] and oxabicycloheptanyl cation. Both follow the Poincaré-Hopf relationship. It also shows some delocalization indices and atomic charges. The electronic nature of the three center-two electron (3c-2e) bonding system in 2-norbornyl and that from oxabicycloheptanyl

Table 1. Geometrical (angle (degree) and bond length (Å)) and topological properties (charge density (ρ_b), Laplacian of charge density ($\nabla^2\rho_b$), atomic energy ($E_{at}(\Omega)$), sum of atomic energies of C1–C3 ($\Sigma E_{at}(\Omega)$) (in a.u.), ellipticity (ε), ratio $|\lambda_1|/\lambda_3$ of the bond critical points (BCP 1-4), delocalization indices (DI) and QTAIM bond orders (n) of their corresponding atomic pairs) of the species **1-GS**, **2-GS**, **1-TS** and **2-TS**

Property		Species			
		1-GS	**1-TS**	**2-GS**	**2-TS**
Angle /degree	C1–C2–C3	109.5	107.3	104.1	92.6
Bond length / Å	C1–C2	1.542	1.584	1.551	1.617
	C2–C3	1.519	1.448	1.508	1.440
	C3–O	1.555	2.300	1.587	2.156
DI[a]	DI(1)	0.966	0.877	0.943	0.832
	DI(2)	0.054	0.107	0.071	0.185
	DI(3)	0.962	1.109	0.971	1.091
ρ_b / a.u.	BCP 1	0.236	0.207	0.230	0.193
	BCP 2	0.251	0.285	0.257	0.288
	BCP 3	0.166	0.032	0.155	0.042
	BCP 4	0.021	0.013	–	–
n	BCP 1	1.03	0.86	0.99	0.79
	BCP 2	1.13	1.39	1.17	1.41
$\nabla^2\rho_b$ / a.u.	BCP 1	−0.512	−0.384	−0.484	−0.320
	BCP 2	−0.591	−0.768	−0.619	−0.779
	BCP 3	−0.071	0.102	−0.057	0.121
	BCP 4	0.064	0.050	–	–
ε	BCP 1	0.015	0.029	0.013	0.074
	BCP 2	0.006	0.063	0.019	0.065
$|\lambda_1|/\lambda_3$	BCP 3	0.640	0.209	0.614	0.216
	BCP 4	0.243	0.181	–	–
$E_{at}(\Omega)$ / a.u.	C1	−38.0222	−38.0109	−38.0214	−38.0251
	C2	−38.0455	−38.0464	−38.0465	−38.0595
	C3	−37.9063	−38.0490	−37.9290	−38.0438
	Σ	−113.9740	−114.1063	−113.9969	−114.1284

[a]DI(1): C1–C2, DI(2):C1–C3 and DI(3): C2–C3.

DI(C1-C2)= 0.54
DI(C1-C3)= 0.54
DI(C3-C2)= 1.22

DI(C1-C2)= 0.11
DI(C1-C3)= 0.88
DI(C3-C2)= 1.01
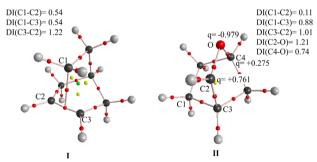DI(C2-O)= 1.21
DI(C4-O)= 0.74

Figure 5. Molecular graph of 2-norbornyl cation (I) and oxabicycloheptanyl cation (II) and some delocalization indices and atomic charges.

cation is different. DI between C2 and O is higher than DI between C4 and O. The latter corresponds to a bond order smaller than a single bond (BO = 0.83) and the former corresponds to a bond order slightly higher than a single bond (BO = 1.04), according to the linear relation between formal bond order and delocalization index[54] (see Supplementary Information).

Discussion

Figure 1 shows that the activation energy of the first step of the nucleophilically unassisted solvolysis of protonated 2-*exo*-norbornanol is ten-fold smaller than that from protonated 2-*endo*-norbornanol. Nevertheless, there is no steric hindrance between the hydrogen atom (bonded to C1 atom) and the oxygen atom of the leaving group in **1-TS**. In truth, there is a bond path between these atoms which indicates a weak attractive interaction involving them (Figure 2). The values of the charge density, the Laplacian of the charge density and the ratio $|\lambda_1|/\lambda_3$ of BCP 4 indicate a closed shell interaction between these atoms (Table 1).

In the solvolysis of the protonated of 2-*endo/exo*-norbornanols, there is an elongation of C1–C2 bond length and decrease of C1–C2–C3 angle from **1-GS** and **2-GS** to **1-TS** and **2-TS**, respectively. These changes are

Table 2. Geometrical (angle (degree) and bond length (Å)) and topological properties (charge density (ρ_b), Laplacian of charge density ($\nabla^2\rho_b$), atomic energy ($E_{at}(\Omega)$), atomic charge ($q(\Omega)$), sum of atomic energies of C1–C3 ($\Sigma E_{at}(\Omega)$) (in a.u.), ellipticity (ε), ratio $|\lambda_1|/\lambda_3$ of the bond critical points (BCP 1-3, 5 and 6) and delocalization indices (DI) of their corresponding atomic pairs) of the species **3-GS**, **4-GS**, **3-TS** and **4-TS**

Property		Species			
		3-GS	**3-TS**	**4-GS**	**4-TS**
Angle / degree	O2–C2–C3	98.9	77.5	96.6	107.6
	C1–C2–C3	110.6	117.5	110.8	88.3
Bond length / Å	C1–C2	1.540	1.516	1.531	1.658
	C2–C3	1.540	1.471	1.526	1.429
	C3–O1	1.542	2.099	1.539	2.309
	O2–C2	1.409	1.459	1.439	1.387
	O2–C3	2.241	1.834	2.214	2.273
DI[a]	DI(1)	0.938	0.966	0.946	0.751
	DI(2)	0.050	0.041	0.050	0.235
	DI(3)	0.904	0.942	0.918	1.078
	DI(4)	0.126	0.502	0.110	0.113
ρ_b / a.u.	BCP 1	0.236	0.251	0.244	0.180
	BCP 2	0.251	0.274	0.255	0.299
	BCP 3	0.166	0.048	0.178	0.030
	BCP 5	0.272	0.236	0.252	0.285
	BCP 6	0.240	0.217	0.235	0.251
$q(\Omega)$ / a.u.	C1	−0.045	−0.017	−0.025	−0.105
	C2	+0.489	+0.377	+0.416	+0.522
	C3	+0.234	+0.139	+0.243	+0.069
	O2	−0.966	−0.807	-0.982	−0.984
$\nabla^2\rho_b$ / a.u.	BCP 1	−0.512	−0.592	−0.554	−0.257
	BCP 2	−0.592	−0.712	−0.606	−0.828
	BCP 3	−0.071	0.135	−0.125	0.098
	BCP 5	−0.564	−0.359	−0.486	−0.582
	BCP 6	−0.532	−0.355	−0.400	−0.443
ε	BCP 1	0.015	0.011	0.017	0.121
	BCP 2	0.006	0.012	0.031	0.096
	BCP 5	0.056	0.256	0.077	0.071
	BCP 6	0.002	0.059	0.061	0.045
$|\lambda_1|/\lambda_3$	BCP 3	0.640	0.221	0.730	0.180
	BCP 5	1.163	1.109	1.163	1.093
	BCP 6	1.091	1.066	1.070	1.047
$E_{at}(\Omega)$ / a.u.	C1	−38.0208	−38.0169	−38.0174	−38.0288
	C2	−37.7423	−37.8495	−37.8029	−37.7408
	C3	−37.8885	−37.9750	−37.8909	−38.0496
	Σ	−113.6516	−113.8414	−113.7112	−113.8192

[a]DI(1): C1–C2, DI(2):C1–C3, DI(3): C2–C3 and DI(4): O2–C3.

higher from **2-GS** to **2-TS** than from **1-GS** to **1-TS**. These geometrical changes are due to the sigma bond participation of C1–C2 bond to C3 atom in the transition state (Table 1). Besides, there is a lengthening of C3–O bond from the

ground state to the transition state in the solvolysis of the protonated 2-*endo*-oxabicycloheptanol.

The values of DI(2) indicate that there is a sigma bond participation in both protonated systems. However, the

increase of DI(2) from **2-GS** to **2-TS** is two-fold higher than that from **1-GS** to **1-TS**. Consequently, the decrease of DI(1) from **2-GS** to **2-TS** is higher than that from **1-GS** to **1-TS**. The charge density and the Laplacian of the charge density of BCP 1 follow the same trend. The increase of DI(3) is nearly similar for both reactions from the ground state to the transition state, being supported by the charge density, the Laplacian of the charge density and the bond order of BCP 2. The sum of the atomic energy of C1−C3 atoms in **2-TS** is smaller than that from **1-TS**. This indicates that the sigma bond participation stabilizes more effectively the forming 3c-2e bond system in **2-TS** than in **1-TS** (Table 1).

In the case of 2-oxabicycloheptanol, the activation energy of the first step of the nucleophilically unassisted solvolysis of protonated 2-*endo*-oxabicycloheptanol is moderately smaller than that from protonated 2-*exo*-oxabicycloheptanol.

Figure 4 shows the difference of geometry of the oxabicycloheptanyl moiety between **3-TS** and **4-TS**. The O2−C3 interatomic distance considerably decreases from **3-GS** to **3-TS**, while slightly increases from **4-GS** to **4-TS** (Table 2). The C1−C2−C3 angle reasonably decreases from **4-GS** to **4-TS** and moderately increases from **3-GS** to **3-TS**. The C1−C2 bond length decreases from **3-GS** to **3-TS** and increases from **4-GS** to **4-TS**. These geometrical changes in the oxabicycloheptanyl moiety from the ground state to the transition state, along with the elongation of the C3−O1 bond, are consequence of considerable anchimeric assistance in the transition state of both protonated systems.

Unlike **1-TS** and **2-TS**, there is no sigma bond participation from C1−C2 bond to C3 atom in **3-TS** because DI(1) slightly increases and DI(2) slightly decreases from **3-GS** to **3-TS**. On the other hand, from **4-GS** to **4-TS** there is a considerable decrease of DI(1) and increase of DI(2), indicating sigma bond participation from C1−C2 atoms in **4-TS**. The charge density and the Laplacian of the charge density of BCP 1 for both protonated systems follow the same trend as their corresponding DI(1) values.

The sigma bond delocalization in **4-TS** is higher than that in **2-TS** because the difference of values of DI(1) and DI(2) from **4-GS** to **4-TS** [$\Delta(DI(1))_{4GS-4TS} = 0.195$ and $\Delta(DI(2))_{4GS-4TS} = -0.185$] is higher than those from **2-GS** to **2-TS** [$\Delta(DI(1))_{2GS-2TS} = 0.111$ and $\Delta(DI(2))_{2GS-2TS} = -0.114$]. Nevertheless, the activation energy from **3-GS** to **3-TS** is 1.64 kcal mol^{-1} smaller than that from **4-GS** to **4-TS** (Figure 3) which means that the anchimeric assistance in **3-TS** is higher than that in **4-TS**. Accordingly, the sum of the atomic energies of C1−C3 atoms of **3-TS** is smaller than that from **4-TS** (Table 2). The higher anchimeric assistance in **3-TS** can be explained by the high increase of DI(4) from

3-GS to **3-TS** (Table 2). The difference of DI(4) value from **3-GS** to **3-TS** [$\Delta(DI(4))_{3GS-3TS} = -0.376$] is higher than the difference of DI(2) value from **4-GS** to **4-TS**.

Moreover, the anchimeric assistance in **3-TS** and **4-TS** can be analyzed by charge densities of BCP and atomic charges. BCP 5 and 6 belong to the bond paths which link O2 atom to C2 and C4 atoms, respectively. The values of the charge density and the Laplacian of the charge density of BCP 5 and 6 decrease in magnitude from **3-GS** to **3-TS**. The ellipticities of BCP 5 and 6 moderately increase. Thus, there is sigma bond participation from O2−C4 and O2−C2 bonds to the C2 and C3 atoms. In addition, there must be valence shell electron participation from O2 atom to C3 atom because the atomic charge of the O2 atom reasonably becomes less negative and the atomic charge of C3 atom becomes less positive from **3-GS** to **3-TS** (Table 2). In the case of **4-TS**, there is no valence shell electron participation from O2 atom because there is no significant change of its atomic charge from **4-GS** to **4-TS**. However, there is a reasonable sigma bond participation from C1−C2 atoms in **4-TS** because the atomic charge of C2 becomes more positive and the atomic charge of C3 atom becomes less positive.

The bond paths involving C1, C2 and C3 atoms of the molecular graphs of **1-TS**, **2-TS**, **3-TS** and **4-TS** are different from their corresponding intermediates 2-norbornyl and oxabicycloheptanyl cations (Figure 5). In addition, the DI values involving C1, C2 and C3 atoms of **1-TS**, **2-TS**, **3-TS** and **4-TS** are very different from those from their corresponding intermediates 2-norbornyl and oxabicycloheptanyl cations (Figure 5). Then, QTAIM analysis confirms Winstein´s hypothesis,[26] later supported by Schleyer and co-workers,[33] that "carbon bridging lags behind ionization at the transition state" in the solvolysis of 2-norbornyl derivatives.

To sum up, the QTAIM results show that, in the first step of the nucleophilically unassisted solvolysis of protonated 2-*exo*-norbornanol and of protonated 2-*endo*-norbornanol, both reactions are anchimerically assisted by sigma bond participation, whereas results from molecular orbital theory indicate only sigma bond participation in transition state of the solvolysis of protonated 2-*exo*-norbornanol.[33] Similarly, in the first step of the nucleophilically unassisted solvolysis of protonated 2-*endo*-oxabicycloheptanol and of protonated 2-*exo*-oxabicycloheptanol, the QTAIM results show that both reactions are anchimerically assisted: the former from sigma bond participation from O−C bonds and valence shell electron participation from oxygen atom and the latter from sigma bond participation from C1−C2 bond. Molecular orbital theory indicates only valence shell electron participation from oxygen atom in the transition state of the solvolysis of protonated 2-*endo*-oxabicycloheptanol.[33]

Conclusions

There is a great correspondence between the differences of energy barrier and the difference of delocalization index that can account for the existence of anchimeric assistance.

The activation energy of the first step of the nucleophilically unassisted solvolysis of protonated 2-*exo*-norbornanol is ten-fold smaller than that from protonated 2-*endo*-norbornanol where both reactions are anchimerically assisted by sigma bond participation from C1–C2 bond to C3 atom, according to QTAIM results. Previous calculations from molecular orbital theory show no sigma bond participation in the transition state of protonated 2-*endo*-norbornanol. However, from QTAIM results, the sigma bond participation in the transition state of protonated 2-*exo*-norbornanol is two-fold higher than that in the former.

The activation energy of the first step of the nucleophilically unassisted solvolysis of protonated 2-*endo*-oxabicycloheptanol is slightly smaller than that of protonated 2-*exo*-oxabicycloheptanol. This is explained (from QTAIM results) by a higher difference of DI(4) value from the protonated 2-*endo*-oxabicycloheptanol ground state to the transition state of protonated 2-*endo*-oxabicycloheptanol than the difference of DI(2) value from the protonated 2-*exo*-oxabicycloheptanol ground state to the transition state of protonated 2-*exo*-oxabicycloheptanol.

The QTAIM results show that the nucleophilically unassisted solvolysis of protonated 2-*endo*-oxabicycloheptanol and of protonated 2-*exo*-oxabicycloheptanol are anchimerically assisted: the former from sigma bond participation from O–C bonds and valence shell electron participation from oxygen atom and the latter from sigma bond participation from C1–C2 bond. Previous molecular orbital results indicate only valence shell electron participation from oxygen atom in the transition state of protonated 2-*endo*-oxabicycloheptanol.

From the comparison of DI values and molecular graphs between transition structures and corresponding intermediate cations, the QTAIM analysis confirms Winstein´s hypothesis[26] that "carbon bridging lags behind ionization at the transition state" in the solvolysis of protonated 2-norbornanol and protonated 2-oxabicycloheptanol.

Supplementary Information

This supplementary material shows the delocalization index of some single and double CO bonds, computed energy values of species **1-GS** to **4-GS**, **1-TS** to **4-TS**, 2-norbornyl and oxabicyloheptanyl cations, relation between delocalization index of CO bonds and formal bond order and Z matrices of optimized structures. These information are available free of charge at http://jbcs.sbq.org.br as PDF file.

References

1. Winstein, S.; Morse, B. K.; *J. Am. Chem. Soc.* **1952**, *74*, 1133.
2. Winstein, S.; Lindegren, C. R.; Marshall, H.; Ingraham, L. L.; *J. Am. Chem. Soc.* **1953**, *75*, 147.
3. Winstein, S.; Lindegren, C. R.; Ingraham, L. L.; *J. Am. Chem. Soc.* **1953**, *75*, 155.
4. Streitwieser, A.; *Chem. Rev.* **1956**, *56*, 571.
5. Winstein, S.; Trifan, D.; *J. Am. Chem. Soc.* **1952**, *74*, 1147.
6. Winstein, S.; Trifan, D. S.; *J. Am. Chem. Soc.* **1949**, *71*, 2953.
7. Winstein, S.; Trifan, D.; *J. Am. Chem. Soc.* **1952**, *74*, 1154.
8. Walling, C.; *Acc. Chem. Res.* **1983**, *16*, 448.
9. Bentley, T. W.; Bowen, C. T.; Morten, D. H.; Schleyer, P. V. R.; *J. Am. Chem. Soc.* **1981**, *103*, 5466.
10. Schleyer, P. V. R.; *J. Am. Chem. Soc.* **1964**, *86*, 1854.
11. Schleyer, P. V. R.; *J. Am. Chem. Soc.* **1964**, *86*, 1856.
12. Lenoir, D.; Apeloig, Y.; Arad, D.; Schleyer, P. V. R.; *J. Org. Chem.* **1988**, *53*, 661.
13. Grob, C. A.; *Acc. Chem. Res.* **1983**, *16*, 426.
14. Mehta, G.; Padma, S.; *J. Org. Chem.* **1988**, *53*, 4890.
15. Bentley, T. W.; Schleyer, P. V. R.; *J. Am. Chem. Soc.* **1976**, *98*, 7658.
16. Schadt, F. L.; Bentley, T. W.; Schleyer, P. V. R.; *J. Am. Chem. Soc.* **1976**, *98*, 7667.
17. Brown, H. C.; *Acc. Chem. Res.* **1973**, *6*, 377.
18. Brown, H. C.; Schleyer, P. V. R.; *The Nonclassical Ion Problem*; Plenum Press: New York, 1977.
19. Olah, G. A.; *Acc. Chem. Res.* **1976**, *9*, 41.
20. Johnson, S. A.; Clark, D. T.; *J. Am. Chem. Soc.* **1988**, *110*, 4112.
21. Olah, G. A.; Mateescu, G. D.; Wilson, L. A.; Gross, M. H.; *J. Am. Chem. Soc.* **1970**, *92*, 7231.
22. Olah, G. A.; White, A. M.; Demember, J. R.; Commeyra, A; Lui, C. Y.; *J. Am. Chem. Soc.* **1970**, *92*, 4627.
23. Olah, G. A.; Prakash, G. K. S.; Arvanaghi, M.; Anet, F. A. L.; *J. Am. Chem. Soc.* **1982**, *104*, 7105.
24. Roberts, J. D.; Mazur, R. H.; *J. Am. Chem. Soc.* **1951**, *73*, 3542.
25. Olah, G. A.; Prakash, G. K. S.; Saunders, M.; *Acc. Chem. Res.* **1983**, *16*, 440.
26. Winstein, S.; *J. Am. Chem. Soc.* **1965**, *87*, 381.
27. Saunders, M.; Kates, M. R.; *J. Am. Chem. Soc.* **1983**, *105*, 3571.
28. Olah, G. A.; White, A. M.; DeMember, J. R.; Commeyras, A.; Lui, C. Y.; *J. Am. Chem. Soc.* **1970**, *92*, 4627.

29. Arnett, E. M.; Petro, C.; Schleyer, P. V. R.; *J. Am. Chem. Soc.* **1979**, *101*, 522.

30. Mueller, P.; Milin, D.; Feng, W. Q.; Houriet, R.; Della, E. W.; *J. Am. Chem. Soc.* **1992**, *114*, 6169.

31. Schleyer, P. V.; Sieber, S.; *Angew. Chem., Int. Ed. Engl.* **1993**, *32*, 1606.

32. Brown, H. C.; *Acc. Chem. Res.* **1983**, *16*, 432.

33. Schreiner, P. R.; Schleyer, P. V.; Schaefer, H. F.; *J. Org. Chem.* **1997**, *62*, 4216.

34. Bader, R. F. W.; *Acc. Chem. Res.* **1985**, *18*, 9.

35. Bader, R. F. W.; *Atoms in Molecules a Quantum Theory*; Oxford University Press: Oxford, 1994.

36. Firme, C. L.; Antunes, O. A. C.; Esteves, P. M.; *J. Phys. Chem. A* **2008**, *112*, 3165.

37. Werstiuk, N. H.; *J. Chem. Theory Comput.* **2007**, *3*, 2258.

38. Werstiuk, N. H.; Muchall, H. M.; *J. Mol. Struct.: THEOCHEM* **1999**, *463*, 225.

39. Werstiuk, N. H.; Muchall, H. M.; *J. Phys. Chem. A* **2000**, *104*, 2054.

40. Fletcher, R.; *Practical Methods of Optimization*, vol. 1; John Wiley and Sons: New York, 1980.

41. Dunning, J. T. H.; *J. Chem. Phys.* **1989**, *90*, 1007.

42. Ernzerhof, M.; Scuseria, G. E.; *J. Chem. Phys.* **1999**, *110*, 5029.

43. Frisch, M. J.; Trucks, G. W.; Schlegel, H. B.; Scuseria, G. E.; Robb, M. A.; Cheeseman, J. R.; Zakrzewski, V. G.; Montgomery, J. A. J.; Vreven, T.; Kudin, K. N.; Burant, J. C.; Millam, J. M.; Iyengar, S. S.; Tomasi, J.; Barone, V.; Mennucci, B.; Cossi, M.; Scalmani, G.; Rega, N.; Petersson, G. A.; Nakatsuji, H.; Hada, M.; Ehara, M.; Toyota, K.; Fukuda, R.; Hasegawa, J.; Ishida, M.; Nakajima, T.; Honda, Y.; Kitao, O.; Nakai, H.; Klene, M.; Li, X.; Knox, J. E.; Hratchian, H. P.; Cross, J. B.; Adamo, C.; Jaramillo, J.; Gomperts, R.; Stratmann, R. E.; Yazyev, O.; Austin, A. J.; Cammi, R.; Pomelli, C.; Ochterski, J. W.; Ayala, P. Y.; Morokuma, K.; Voth, G. A.; Salvador, P.; Dannenberg, J. J.; Zakrzewski, V. G.; Dapprich, S.; Daniels, A. D.; Strain, M. C.; Farkas, O.; Malick, D. K.; Rabuck, A. D.; Raghavachari, K.; Foresman, J. B.; Ortiz, J. V.; Cui, Q.; Baboul, A. G.; Clifford, S.; Cioslowski, J.; Stefanov, B. B.; Liu, G.; Liashenko, A.; Piskorz, P.; Komaromi, I.; Martin, R. L.; Fox, D. J.; Keith, T.; Al-Laham, M. A.; Peng, C. Y.; Nanayakkara, A.; Challacombe, M.; Gill, P. M. W.; Johnson, B.; Chen, W.; Wong, M. W.; Gonzalez, C.; Pople, J. A.; Gaussian 03, Revision B.04; Gaussian. Inc.: Pittsburgh, 2003.

44. Biegler-König, F.; Schönbohm, J.; AIM2000-A, Program to Analyze and Visualize Atoms in Molecules, version 2.0, 2002.

45. Bader, R. F. W.; Beddall, P. M.; *J. Chem. Phys.* **1972**, *56*, 3320.

46. Bader, R. F. W.; Beddall, P. M.; *J. Am. Chem. Soc.* **1973**, *95*, 305.

47. Bader, R. F. W.; Stephens, M. E.; *J. Am. Chem. Soc.* **1975**, *97*, 7391.

48. Bader, R. F. W.; Beddall, P. M.; Cade, P. E.; *J. Am. Chem. Soc.* **1971**, *93*, 3095.

49. Srebrenik, S.; Bader, R. F. W.; *J. Chem. Phys.* **1975**, *63*, 3945.

50. Bader, R. F. W.; *Acc. Chem. Res.* **1975**, *8*, 34.

51. Bader, R. F. W.; Srebrenik, S.; Nguyendang, T. T.; *J. Chem. Phys.* **1978**, *68*, 3680.

52. Bader, R. F. W.; Streitwieser, A.; Neuhaus, A.; Laidig, K. E.; Speers, P.; *J. Am. Chem. Soc.* **1996**, *118*, 4959.

53. Bader, R. F. W.; Tang, T. H.; Tal, Y.; Biegler-könig, F. W.; *J. Am. Chem. Soc.* **1982**, *104*, 946.

54. Firme, C. L.; Antunes, O. A. C.; Esteves, P. M.; *Chem. Phys. Lett.* **2009**, *468*, 129.